HHS Public Access

Author manuscript

Neuroimage Rep. Author manuscript; available in PMC 2022 December 23.

Published in final edited form as:

Neuroimage Rep. 2022 December ; 2(4): . doi:10.1016/j.ynirp.2022.100132.

Phase matters when there is power: Phasic modulation of corticospinal excitability occurs at high amplitude sensorimotor mu-oscillations

Recep A. Ozdemir[a,b,*], **Sofia Kirkman**[a], **Justine R. Magnuson**[a,b], **Peter J. Fried**[a,b], **Alvaro Pascual-Leone**[b,c,d], **Mouhsin M. Shafi**[a,b,**]

[a]Berenson-Allen Center for Noninvasive Brain Stimulation, Department of Neurology, Beth Israel Deaconess Medical Center, Boston, MA, USA

[b]Department of Neurology, Harvard Medical School, Boston, MA, USA

[c]Hinda and Arthur Marcus Institute for Aging Research and Deanne and Sidney Wolk Center for Memory Health, Hebrew Senior Life, Boston, MA, USA

[d]Guttmann Brain Health Institute, Institut Guttmann de Neurorehabilitació, Universitat Autonoma de Barcelona, Badalona, Spain

Abstract

Prior studies have suggested that oscillatory activity in cortical networks can modulate stimulus-evoked responses through time-varying fluctuations in neural excitation-inhibition dynamics. Studies combining transcranial magnetic stimulation (TMS) with electromyography (EMG) and electroencephalography (EEG) can provide direct measurements to examine how instantaneous fluctuations in cortical oscillations contribute to variability in TMS-induced corticospinal responses. However, the results of these studies have been conflicting, as some reports showed consistent phase effects of sensorimotor mu-rhythms with increased excitability at the negative mu peaks, while others failed to replicate these findings or reported unspecific mu-phase effects across subjects. Given the lack of consistent results, we systematically examined the modulatory effects of instantaneous and pre-stimulus sensorimotor mu-rhythms on corticospinal responses with offline EEG-based motor evoked potential (MEP) classification analyses across five identical visits. Instantaneous sensorimotor mu-phase or pre-stimulus mu-power alone did not significantly modulate MEP responses. Instantaneous mu-power analyses showed weak effects with larger MEPs during high-power trials at the overall group level analyses, but this trend was not reproducible across visits. However, TMS delivered at the negative peak of high magnitude mu-oscillations generated the largest MEPs across all visits, with significant differences compared to other peak-phase combinations. High power effects on MEPs were only observed at the trough phase of ongoing mu oscillations originating from the stimulated region, indicating site

[*]Corresponding author. Mouhsin Shafi Berenson-Allen Center for Non-Invasive Brain Stimulation, Beth Israel Medical Center, Harvard Medical School, Boston, MA, USA. rozdemir@bidmc.harvard.edu (R.A. Ozdemir). [**]Corresponding author. Berenson-Allen Center for Noninvasive Brain Stimulation, Department of Neurology, Beth Israel Deaconess Medical Center, Boston, MA, USA. mshafi@bidmc.harvard.edu (M.M. Shafi).

Appendix A. Supplementary data

Supplementary data to this article can be found online at https://doi.org/10.1016/j.ynirp.2022.100132.

and phase specificity, respectively. More importantly, such phase-dependent power effects on corticospinal excitability were reproducible across multiple visits. We provide further evidence that fluctuations in corticospinal excitability indexed by MEP amplitudes are partially driven by dynamic interactions between the magnitude and the phase of ongoing sensorimotor mu oscillations at the time of TMS, and suggest promising insights for (re)designing neuromodulatory TMS protocols targeted to specific cortical oscillatory states.

1. Introduction

Transcranial magnetic stimulation (TMS) has become a primary tool for noninvasive brain stimulation, enabling safe and mechanistic means of perturbing and modulating network-level dynamics with high spatial and temporal specificity (Rossi et al., 2020). TMS of the human motor cortex (M1) generates transsynaptic action potentials along the corticospinal tract and evokes motor potentials (MEPs) at the stimulated muscles. The peak-to-peak MEP amplitude is the most commonly used metric in both basic TMS research and its' clinical applications to index corticospinal excitability (Pascual-Leone et al., 1998), determine TMS dosing (Rothwell et al., 1999), examine corticocortical (Sanger et al., 2001) or corticospinal dynamics (Levy et al., 1984), diagnose clinical/neurological conditions (Di Lazzaro et al., 1999) and evaluate the therapeutic effectiveness of neuromodulatory interventions (Fregni and Pascual-Leone, 2007; Kobayashi and Pascual-Leone, 2003; Lefaucheur et al., 2014).

Despite its widespread experimental and clinical use, however, a landmark feature of MEP amplitudes is their substantial variability between successive trials apart only few seconds, even with constant stimulation parameters and experimental conditions (Goetz et al., 2014; Hordacre et al., 2017; Kiers et al., 1993; Rösler et al., 2008; Wassermann, 2002). A large body of prior research has also demonstrated that there is both high inter- and intra-individual variability (Amassian et al., 1989; Corp et al., 2021; Jung et al., 2010; Pellegrini et al., 2018), although stimulation intensity is assumed to be functionally standardized across subjects and visits. As such, the utility of MEPs as a reliable neurophysiological metric of corticocortical or corticospinal dynamics has been a matter of ongoing debate (Livingston and Ingersoll, 2008; Pellegrini et al., 2018), with a collection of experimental and methodological factors including stimulation parameters, devices, and stimulated muscles contributing to the variability in MEP responses (Corp et al., 2021). Recently, there has been an increased interest in studying instantaneous cortical oscillations under the stimulated region to account for fluctuations in corticospinal excitability (Zrenner et al., 2016), as it has long been suggested that the evoked responses generated by external stimuli depends on the interaction between the neurophysiological state of the brain and external stimulus properties at the time of stimulation (Silvanto and Pascual-Leone, 2008). With the advances in technology, it has become possible to estimate oscillatory state of the brain in real time by monitoring electroencephalographic (EEG) recordings and delivering TMS pulses at the specific phases of cortical oscillations (Bergmann, 2018; Bergmann et al., 2012).

Alpha-band (8–12Hz) oscillations, called mu-rhythms in the sensorimotor cortex, are prominently expressed in sensorimotor cortices and have been shown to modulate voluntary

motor behaviors (Haegens et al., 2011a), perception (Jensen and Mazaheri, 2010), sensorimotor processing (Haegens et al., 2011b), and cortical connectivity (Momi et al., 2022) in a phasic manner through periodical bouts of increased neural excitation and inhibition dynamics, with neuronal membranes closer to action potential threshold at the trough of alpha oscillations (Arieli et al., 1996). Thus, several studies have synchronized single TMS pulses with the dynamics of ongoing mu activity to examine whether instantaneous properties (phase and/or power) of sensorimotor mu-rhythms modulate TMS induced corticospinal excitability, but reported inconsistent results (Bergmann et al., 2019; Desideri et al., 2019; Hussain et al., 2019; Karabanov et al., 2021; Madsen et al., 2019; Schaworonkow et al., 2018, 2019, 2018; Zrenner et al., 2018, 2020). Recent studies by one research group have consistently reported mu phase-dependent modulation of corticospinal excitability with significantly larger MEP amplitudes when TMS is delivered at the negative as compared to the positive peaks of mu oscillations (Bergmann et al., 2019; Schaworonkow et al., 2019; Zrenner et al., 2018). Other groups, however, failed to replicate these results by either showing no phase or power-dependent modulation of MEPs (Madsen et al., 2019), or reported lack of phase consistency for the relationship between mu oscillations and MEP responses (Schilberg et al., 2021). Differences in experimental protocols (number of trials, inter-stimulus intervals etc), EEG preprocessing approaches (surface laplacian or radial source estimation, window sizes used to estimate EEG metrics) and relatively small sample sizes (n ranges from 12 to 27) to detect small or medium effects may all be considered as possible factors contributing to diverging results across different groups. In addition, although trial-to-trial fluctuations in MEP responses are well documented (Rösler et al., 2008), none of these studies systematically analyzed whether instantaneous properties of mu oscillations contributes to MEP response variability across successive trials. More importantly, the reproducibility of either phase- or power-dependent corticospinal excitability across sessions has not been reported in any of the previous studies.

In this study, we aimed to address these knowledge gaps and performed offline EEG based MEP classification analyses across five identical visits. First, we sought to determine whether mu-rhythm phase, power or combination of both derived from the stimulated brain region differently modulates MEP amplitudes in healthy young adults. Second, we performed identical analyses independently across multiple sessions (5 sessions), with sample sizes ranging from 28 to 41, to test the reproducibility and robustness of mu-rhythm effects on MEP amplitudes. Finally, we compared trial-to-trial stability of MEPs in each oscillatory state to provide preliminary insights into effects of murhythm properties on MEP response variability across trials.

2. Methods

Participants:

Forty-one right-handed healthy volunteers (16 males; mean ± SD age = 35.87 ± 15.63 years, range = 19 to 65) participated in this study. None of the participants had self-reported history of psychiatric or neurological diseases. In accordance with the Declaration of Helsinki, experimental protocols and voluntary participation procedures were explained to all participants before they gave their written informed consent to the study. All

questionnaires and procedures were approved by the Institutional Review Board of the Beth Israel Deaconess Medical Center, Boston, MA. All 41 subjects completed first visit (V1), while 36 subjects completed first two visits, 35 subjects completed 3 visits, 33 subjects completed 4 four visits, and 28 subjects were completed all 5 visits.

Data acquisition: A T1-weighted (T1w) anatomical MRI scan was obtained for all participants and used for neuronavigation. MRI data were acquired on a 3T scanner (GE Healthcare, Ltd.) using a three-dimensional spoiled gradient echo sequence: 166 axial-oriented slices for whole-brain coverage; 240-mm isotropic field-of-view (FOV); 0.937-mm × 0.937-mm × 1-mm native resolution; flip angle = 15°; echo time (TE)/repetition time (TR) ≥ 2.9/6.9 ms; duration ≥432 s.

TMS was delivered using a figure-of-eight–shaped coil with dynamic fluid cooling (MagPro 75-mm Cool B-65; MagVenture A/S) attached to a MagPro X-100 stimulator (MagVenture A/S). Individual high-resolution T1w images were imported into the Brainsight TMS Frameless Navigation system (Rogue Research Inc.), and coregistered to digitized anatomical landmarks for online monitoring of coil positioning.

Auxiliary channels of BrainVision actiCHamp amplifier system (actiCHamp system; Brain Products GmbH) was used to acquire and digitize EMG data at a sampling rate of 5000 Hz. EMG signals were continuously streamed by using BrainVision recorder software (Software Version 1.20.0601, Brain Products GmbH) to monitor MEPs and epochs were recorded with a 150 ms window length covering from 50 ms before to 100 ms after TMS pulse. Motor-evoked potentials (MEPs) were recorded from the right first dorsal interosseous (FDI) muscle. Ag–AgCl surface electrode pairs were placed on the belly and tendon of the muscle and a ground was placed on the right ulnar styloid process.

Whole-scalp 64-channel EEG data were collected at a sampling rate of 5000 Hz with a high frequency cut-off at 1350 Hz using a TMS-compatible amplifier system (actiCHamp system; Brain Products GmbH) and labeled in accordance with the extended 10–20 International System. EEG data were online-referenced to AFz electrode. Electrode impedances were maintained below 5 kΩ. EEG signals were digitized using a Brainamp actiCHamp amplifier and linked to BrainVision Recorder software (version 1.21) for online monitoring. Digitized EEG electrode locations on the scalp were also coregistered to individual MRI scans using Brainsight TMS Frameless Navigation system.

Experimental procedures:

Participants underwent five neuro-navigated TMS-EEG-EMG visits that explore cortical plasticity, reactivity, connectivity, and behavioral effects of different rTMS stimulation applied to the left primary motor cortex (M1). Data presented in this study were collected from M1 before the application of any rTMS protocol as a baseline measure of motor cortical excitability (See Fig. 1A for details of experimental design of a given rTMS session). The order of first visits for each rTMS condition was randomized between subjects. Each visit was spaced 1–4 weeks apart to minimize carry over effects, Visits for a given participant were scheduled at the same time of the day as much as possible to control for

circadian fluctuations in cortical excitability. For women, each visit was conducted at the same (luteal) phase of the menstrual cycle (4 weeks apart approximately).

At the beginning of each visit, the motor hotspot was determined over the hand region of left motor cortex (L-M1) for eliciting MEPs in the right FDI muscle. The hotspot was defined as the region where singlepulse TMS elicited consistent MEPs in the FDI muscle. Following International Federation of Clinical Neurophysiology (IFCN) guidelines, resting motor threshold (RMT) was determined on the FDI hotspot as the minimum stimulation intensity eliciting at least five MEPs (0.05 mV) out of ten pulses in the relaxed FDI using biphasic (with the second phase inducing posterior-anterior electric field in the brain) current waveforms (Rothwell et al., 1999). In compliance with the IFCN safety recommendations, participants were asked to wear earplugs during hotspot and RMT trials to protect their hearing, and to minimize external noise (Rossi et al., 2020; Rossini et al., 2015). TMS was administered with a thin layer of foam placed under the coil to minimize TMS-related vibration artifacts in EEG responses. To minimize auditory evoked potentials related to the TMS coil click, auditory white noise masking was presented through earplug-earbuds at the maximum volume comfortable for each participant.

Following determination of motor thresholds in each session, 150 single pulses of TMS (spTMS) at 120% of RMT were delivered to the motor hotspot with 3–5s randomly jittered inter-stimulus intervals as a baseline measure of corticospinal (MEPs) excitability.

EMG preprocessing:

EMG data were band-pass filtered (10–2000 Hz) for offline analyses and each trial is baseline corrected (Pre TMS) by subtracting the mean value of 45 ms period (−50 ms to −5 ms) before TMS from the entire signal (Fig. 1B). Root mean square (RMS) of baseline signal is computed from −20 to 13 ms (omitting −2 to 2 ms period to exclude any TMS artifacts) to identify trials with artifacts and potential muscle contractions. Trials with baseline RMS values 2.5 SD above the average RMS of the entire block is discarded (Fig. 1C). Following removing of trials with high baseline RMS, peak-to-peak MEPs were computed as the absolute difference between maximum and minimum voltage values from 20 ms–50 ms following TMS for each trial. Furthermore, trials with peak-to-peak MEPs above or below 2.5 SD of the average MEP of the block are identified as outliers and removed from the data (See Fig. 1B, C and D for the illustration of EMG preprocessing).

EEG preprocessing:

All EEG data pre-processing was performed offline using EEGLAB 20.1 (Delorme and Makeig, 2004), and customized scripts running in Matlab R2020b (Math-Works Inc., USA). EEG data were first segmented into 2000 ms epochs preceding TMS pulse (−2000 ms 0 ms) for each trial. Epochs were visually inspected to check if any TMS artifact present at 0 ms. In case of remaining TMS artifacts at 0 ms (less than 10% of subjects in all visits) epochs were zero padded up to 2 ms preceding TMS (−2 to 0 ms corresponding to 10 samples) and then interpolated using linear interpolation. Another visual inspection is performed to identify and reject extremely noisy channels (2.22 ± 1.92 channels were deleted on average; range 0–6 out of 63). Following Channel rejection, epochs were then tagged

based on voltage (≥100 mV), kurtosis (≥3), and joint probability (Single channel based threshold ≥3.5sd; All channel-based threshold ≥ 5sd) metrics to identify excessively noisy epochs. Visual inspection was performed on the tagged epochs for the final decision for the removal of noisy epochs (8.27 ± 7.31) epochs were deleted on average; range 0–46 out of 150). EEG data were then notch filtered between 57 and 63Hz, band pass filtered using a forward-backward 4^{th} order Butterworth filter from 1 to 50Hz, and referenced to global average. To avoid edge effects of the Butterworth filter at individual epochs, each epoch is first replicated, inverted and then reflected back to both ends of the signal for symmetrical extension of the original epoch before filtering. Original epochs were then extracted back following the filtering process for further processing steps. A fast independent component analysis (fICA) was performed to manually remove all remaining artifact components including eye movement/blink, muscle noise (EMG), single electrode noise, and cardiac beats (EKG) (see Ozdemir et al., 2021, 2020 for details of identifying ICA components). A semi-automated artifact detection algorithm "tesa_compselect" incorporated into the open source TMS-EEG Signal Analyzer (TESA v0.1.0-beta (Rogasch et al., 2017)) extension for EEGLAB was used to visually inspect and manually remove artifactual resting-state EEG ICA components based on their frequency, activity power spectrum, amplitude, scalp topography, and time course (http://nigelrogasch.github.io/TESA/). In average, 35.53 ± 7.02 out of 63 ICA components were removed across all data sets and visits (See Supplementary Fig. 1 for visual illustration of artifactual and neural components from a representative subject).

Instantaneous EEG Phase and Power:

A Hjorth-style surface laplacian (Hjorth, 1975) transformation was performed to preprocessed EEG data to control for volume condition effects and attenuate signal contribution from distant sources. In particular, each trial was Hjorth-transformed using electrodes over the left sensorimotor region, with C3 as the central electrode and FC1, FC5, CP1, CP5 as surrounding electrodes (Ermolova et al., 2021; Schaworonkow et al., 2019; Zrenner et al., 2018) to better isolate local cortical oscillations over the stimulated region (Fig. 2A). Hjorth-transformed C3 signal was concatenated across trials and power spectral density was estimated using the welch method ("pwelch" function in Matlab with 1000 ms Hamming window and with %50 overlap ratio). Peak alpha frequency (PAF) was calculated as the frequency point with highest power between 8 and 12Hz for each individual. Hjorth-transformed C3 signal was then band pass filtered around individual PAF (±2 Hz). Finally, Instantaneous phase and power were estimated by computing the analytic signal of the Hjorth-transformed C3 signal using a fast Fourier transform (FFT)-based Hilbert transform for each trial (Fig. 2A). Individual epochs were symmetrically extended before band-pass filtering, as described above, and extracted-back following Hilbert transform to avoid edge artifacts. Trials with phase angles between 330°-30° were classified as "peak", while trials with phase angles between 150°−210° were classified as "trough" trials. All other trials with phase angles between 210° −330°, and between 30° −150° were classified as "null phase" trials. Instantaneous power of the Hjorth-transformed C3 signal was averaged over 100 ms preceding TMS pulse to cover approximately one full cycle of mu oscillations. Trials with power values above 80^{th} percentile were classified as "high-power" and trials with power values below 20^{th} percentile were classified as "low-power", and all other trials with power

values between 20^{th}-80^{th} percentiles were classified as "null power" trials. To classify MEP trials as a combination of EEG phase and power, four categories were generated as follows: Trials with high power (>80%) at the positive peak (high-peak), trials with high power at the negative peak (high-trough), trials with low power (<20%) at the positive peak (low-peak), and trials with low power at the negative peak (low-trough).

Pre-stimulus Power Spectral Density:

In addition to instantaneous power calculation with Hjorth-transformed C3 signal, spectral power density of each EEG electrode was also computed for individual trials using the welch method with hamming windows (1000 ms) and 50% overlap (Fig. 2B). Local PSD at the stimulated region is estimated by averaging power from the same channels used for Hjorth transformation (C3, FC1, FC5, CP1 and CP5). Pre-stimulus (−2000 ms–0 ms) mu power for each trials was extracted by averaging power values between 8 and 12 Hz. Trials with power values above 80^{th} percentile were classified as "high power" and trials with power values below 20^{th} percentile were classified as "low power", and all other trials with power values between 20^{th}-80^{th} percentiles were classified as "null power" trials.

Statistical Analyses:

Accuracy of Mu phase estimation at the time of TMS was assessed with V-tests for circular uniformity using circular statistics toolbox in Matlab (Berens, 2009). Expected mu phase angle was 0° and 180° for peak and trough trials, respectively. The Watson–Williams test was performed to compare differences in average angles across phase conditions (Berens, 2009). For the main analyses, out of 25,950 possible MEP trials, a total of 21,628 MEP trials (125.02 trials per subject in average) were analyzed resulting in 16.66% rejection rate across all visits and subjects. For our main analyses, due to the offline design of our study, we noticed substantial differences in the number of MEPs classified as a function of EEG phase and power across subjects within a single session, and across visits within the same subject (ranging from 1 to 36 trials in each bin per subject per session). Therefore, we first pooled log transformed normalized MEPs across all visits for each subject, with the main goal of examining whether MEPs were statistically different across phase and power conditions at the group level. For each subject, mean MEP amplitude of the block (block-mean) was computed and each MEP trial was normalized to the block mean as percent change and log-transformed for statistical analyses to reduce skew (Lahr et al., 2016). For a given subject, if the total number of individual trials for any phase, power and combination of phase and power (phaseXpower) conditions were 2.5 standard deviation below the average number of trials across all subjects, we excluded that subject's data from the analyses. Applying the above criteria we ended up with total of 4325 single MEP trials both for high power and low power and 12978 MEPs in the null power condition across all subjects and visits. For phase analyses we included 3759, 3165, and 14704 MEP trials for peak, trough and null phase conditions, respectively. For phase and power combinations we included a total of 4808 MEP trials (1257 for low-trough, 1213 for low-peak, 1311 for high-trough and 1027 for high-peak conditions). We then performed repeated-measure analyses of variance (Rm-ANOVAs) with *phase* (trough, peak, null), *power* (high, low, null) and *phaseXpower* (high-trough, high-peak, low-trough, low-peak) conditions as within-subject factors. To break down significant group effects in each Rm-ANOVA, we performed follow-up paired

sample t-tests with Bonferroni corrections to control for multiple comparisons. In addition to pooled analyses, we also performed the same Rm-ANOVAs for each visit separately to examine whether we could reproduce any of the overall group effects observed in our pooled analyses across visits with an independent set of analyses. We also performed intra class correlation (ICCs) using the average MEP values for each subject to further examine consistency of MEP amplitudes for each condition across visits. ICCs <.25 were considered as “very low”, between 0.25 and 0.50 were considered as “low”, between 0.50 and 0.75 were considered as moderate, and >0.75 were considered as “high” reproducibility, respectively (McGraw and Wong, 1996).

3. Results

3.1. Distribution of estimated mu phases

The grand average of Hjorth transformed C3 time series, scalp distribution of average EEG activity, and angular distribution of phase estimation at the time of TMS for each trial across sessions are provided in Fig. 3. The grand average EEG voltage in Hjorth transformed C3 at the time of TMS was 2.62μ (±1.29) for positive peaks, −2.19μ (±1.71) for negative peaks, and −0.14 (±0.52) for null peaks, respectively (Fig. 3A). Scalp EEG topographies averaged across trials and visits showed highly localized activity over left sensorimotor regions for mu peaks and troughs but not for null phase trials (Fig. 3B). We performed V-tests to statistically assess uniformity of phase angle distributions clustered around 0° for peak and 180° for trough trials (Fig. 3C). The results of phase angle distributions both for peak and trough trials were statistically uniform with significant clustering around 0° for peak ($V = 4517.08$, $p < 0.0001$, mean phase angle = 4.17) and 180° for trough trials ($V = 4238.65$, $p < 0.0001$, mean phase angle = 183.5°). Additionally, phase angle distributions were significantly different between peak and trough trials (Peak vs Trough: $t_{(1, 8924)} = 47.278$, $p < 0.000$). Altogether, our control analyses confirmed accuracy of our oscillatory phase estimations by showing uniformly clustered EEG phase values around expected angles, reflecting expected polarity in the EEG topography, and having significant differences between peak and trough phase angles at the time of TMS.

3.2. Corticospinal excitability as function of mu phase

The grand average MEP time series and distribution of normalized MEP averages for each subject were provided in Fig. 3D. For overall group level phase analyses, one subject is excluded from the analyses due to insufficient number trials across visits. When classified as a function of mu-phase alone, no significant differences were observed ($F_{(2,38)} = 1.761$, $p = 0.091$, $\eta_p^2 = 0.11$, power = .475) among null, peak and trough phase MEPs (Fig. 3D, light panel) with grand average of normalized trough phase MEPs (mean = 1.16 ± 3.82%) negligibly larger than peak phase MEPs (mean = −1.13 ± 3.91%). To compare MEP amplitudes across multiple phase bins, we then classified MEPs at 60° phase bins (330–30, 30–90, 90–150, 150–210, 210–270 and 270–330) averaged across all sessions and subjects (Supplementary Fig. 2A). MEP amplitudes were not statistically different from each other across different phase bins ($F_{(5,36)} = 1.568$, $p = 0.087$, $\eta_p^2 = 0.09$, power = .415) although

negative phase bin (blue region in Supplementary Fig. 2A last polar histogram) MEPs were on average (1.4273 mV) higher than the rest of the phase bins.

With a series of control analyses we examined whether our instantaneous phase results are confounded due to potential PAF-filter induced phase distortions at the time of TMS. We first estimated the phase of mu filtered Hjorth channel exactly one PAF cycle before the TMS for each trial (Supplementary Fig. 3A) and called these phases as "Control TMS phase". We then identify actual TMS phases at time zero that are ±60° away from the "Control TMS phase" within the same trial as "potentially artifactual/suspicious trials". We then removed these trials from the final MEP data sets (Supplementary Fig. 3A), and re-performed our main instantaneous phase-based MEP comparisons (Supplementary Fig. 3B). As an alternative control analysis, we also estimated instantaneous muphase 10 samples before the TMS at "−2 ms" (corresponding to a 7.2° phase shift at 10Hz PAF with 5 kHz sampling rate) to avoid possible artifactual phases introduced by mirror padding at time zero. The results of these control analyses in overall was similar to our original analyses with no significant MEP amplitude differences across different phase windows in both control analyses (Control TMS phase: $F_{(2,38)} = 1.215$, p = 0.107, $\eta_p^2 = 0.08$, power = .432, and −2 ms phase: $F_{(2,38)} = 1.097$, p = 0.128, $\eta_p^2 = 0.05$, power = .384). These control analyses suggest that our main results for the effect of mu-phase on corticospinal excitability are unlikely to be confounded by the presence of potentially distorted phase estimates at the time of TMS.

3.3. Corticospinal excitability as function of instantaneous and pre-stimulus mu power

Illustration of instantaneous EEG power and pre-TMS power based classification of MEPs are provided in Fig. 4. For overall group level power analyses, one subject is excluded from the analyses due to insufficient number trials across visits. Rm-ANOVA showed a significant condition effect for instantaneous power differences ($F_{(2,38)} = 394.461$, p = 0.000, $\eta_p^2 = 0.38$, power = 1.000), with high power (mean = 37.30 ± 41.13) having significantly greater mu power than the null power group (mean = 18.23 ± 27.63), and the null power having significantly greater mu power than the low power condition (mean = 8.92 ± 17.63). Similarly, there was a significant condition effect for EEG pre-stim spectral power comparisons ($F_{(2,38)} = 27.154$, p = 0.000, $\eta_p^2 = 0.11$, power = 0.985) among high (mean = 2.50 ± 2.51), null (mean = 1.48 ± 1.52) and low pre-stim (mean = 0.53 ± 0.70) power groups. Rm-ANOVA results for effects of instantaneous power on MEPs showed significant condition effect ($F_{(2,38)} = 5.768$, p = 0.004, $\eta_p^2 = 0.22$, power = .815). Pairwise comparisons revealed MEPs in high power (mean = 4.9 ± 7.01%) were significantly ($p = 0.005$) larger than MEPs in low power (mean = −3.42 ± 6.72%), but not different than MEPs in null power condition (mean = 0.06 ± 4.65%) (Fig. 4A right panel). In contrast, although Rm-ANOVA for pre-stimulus power analyses showed significant main effect for condition ($F_{(2,39)} = 3.514$, p = 0.041, $\eta_p^2 = 0.16$, power = .62), pairwise comparison with bonferroni corrections revealed no significant differences among high (mean = 2.95 ± 7.68%), low (mean = − 3.91 ± 6.38%) and null (mean = 0.37 ± 2.11%) power conditions (Fig. 4B right panel).

We then performed linear regression models to better understand instantaneous mu power and MEP amplitude relationships at “null”, “peak”, “trough” and “all phase bin” conditions using all trials (Supplementary Fig. 2B), and compared the slopes from these models (Supplementary Fig. 2C). While statistically all regression models were significant ($p < 0.001$) due to the sample size, explained variance in MEP amplitudes by instantaneous power were negligible in all models (“all phase trials: $r = 0.023$ and $r^2 = 0.001$, “null phase trials”: $r = 0.021$ and $r^2 = 0.000$; “peak phase trials”: $r = 0.012$ and $r^2 = 0.000$), with highest positive correlation between instantaneous power and MEP amplitude was observed in “trough phase” trials ($r = 0.042$ and $r^2 = 0.002$), and comparison of slopes did not reveal any significant difference ($p > 0.05$)across conditions.

3.4. Corticospinal excitability as function of instantaneous phase and power interactions

Next, MEPs were classified at different levels of instantaneous mu phase and power (Fig. 5A and B). We excluded 8 subjects from the overall group level analyses due to insufficient MEP trials across sessions compared to the rest of the group. Rm-ANOVA showed significant condition effect ($F_{(3,30)} = 6.491$, p = 0.000, $\eta_p^2 = 0.39$, power = 0.934) with pairwise comparisons revealing high-trough MEPs (mean = 9.27 ± 9.88%) significantly larger than high-peak (mean = −7.93 ± 8.54%, $p = 0.000$), MEPs (Fig. 5C, right panel).

To investigate spatial specificity of instantaneous mu phase and power effects, we then classified MEPs as a function of posterior alpha oscillations with POz as the central electrode and P1, P2, O1 and O2 as neighboring electrodes for Hjorth and Hilbert transformations (Supplementary Fig. 4). No significant MEP amplitude differences were observed ($p > 0.05$) for any combination of posterior alpha power and phase oscillations (Supplementary Fig. 4), suggesting that modulation of corticospinal excitability is specific to dynamics of sensorimotor mu oscillations. To investigate phase specificity of high power effects we observed in Fig. 5C, we classified MEPs as a function of rising (240°−300°) and falling phase (60°−120°) bins at high and random power conditions (Supplementary Fig. 5) Although MEP amplitudes at rising phase high power condition were slightly higher (mean = 5.21 ± 6.18%) than falling phase high power condition (mean = −0.24 ± 4.36%), no statistical difference was observed between conditions ($F_{(1,39)} = 1.452$, p = 0.097, $\eta_p^2 = 0.02$, power = .489), suggesting modulation of corticospinal excitability is specific to high-trough (Fig. 5C) condition. To assess the stability of instantaneous power at peak and trough phases we compared instantaneous sensorimotor mu power between high-trough versus high-peak conditions and the low-trough versus low-peak conditions (Supplementary Fig. 6). Paired sample t-tests (low trough vs low peak and high trough vs high peak) were not significant for both comparisons ($p > 0.05$), suggesting that instantaneous mu power was not different across peak and trough phase bins.

3.4.1. Reproducibility of brain state effects on corticospinal excitability—

We then performed identical analyzes with MEPs separately for each visit to examine whether significant results for instantaneous power (Fig. 4A, right panel) and phase dependent power effects (Fig. 5C, right panel) at the overall group level analyses are reproducible across individual sessions independently. For instantaneous power, only significant condition effect was found in visit-2 ($F_{(2,34)} = 4.407$, p = 0.024, $\eta_p^2 = 0.11$, power = 0.643), however pairwise

comparisons with bonferroni corrections did not show any significant differences among instantaneous power conditions. On the other hand, we observed very similar MEP response patterns for phase dependent power effects with significant condition effects at 4 out of 5 visits (Visit-1: $F_{(3,38)} = 4.592$, p = 0.029, $\eta_p^2 = 0.27$, power = 0.870, Visit-2: $F_{(3,33)} = 3.941$, p = 0.031, $\eta_p^2 = 0.24$, power = 0.846, Visit-4: $F_{(3,32)} = 6.994$, p = 0.001, $\eta_p^2 = 0.41$, power = 0.987, Visit-5: $F_{(3,25)} = 5.764$, p = 0.004, $\eta_p^2 = 0.41$, power = 0.912). Pairwise comparisons with bonferroni corrections revealed that high-trough MEPs were significantly larger than high-peak MEPs at visits 1, 2 and 5 ($p = 0.025$, 0.017, and 0.016, respectively); low-peak MEPs at visits 1, 2 and 4 ($p = 0.033$, 0.017 and 0.020, respectively); and low-trough MEPs at visits 1 and 4 ($p = 0.042$ and 0.011, respectively) (Fig. 6). Although, high-trough MEPs in average were larger than other phase-power combinations, no significant condition effect was found in Visit-3 (Visit-3: $F_{(3,32)} = 3.116$, p = 0.051, $\eta_p^2 = 0.20$, power = 0.649).

We performed a series of control analyses to examine whether the different statistical results at separate visits could be due to changes motor hot spot across visits, targeting error due to coil positioning or systematic coil drifts across trials (Supplementary Fig. 7). No significant deviations ($p > 0.05$) within individual subjects in motor hot spot locations were found across visits (Supplementary Fig. 7A). Average target error from the motor hot-spot was between 3 and 5 mm (Supplementary Fig. 7B) and with no significant differences across session ($F_{(4,80)} = 1.522$, p = 0.21, $\eta_p^2 = 0.07$, power = .45). Similarly, paired average targeting error comparisons between the first and last 25 trials for each visit was not-significant (Visit 1: $t_{(26)} = 0.275$, $p = 0.78$, Visit 2: $t_{(22)} = -1.909$, $p = 0.07$, Visit 3: $t_{(26)} = -0.772$, $p = 0.447$, Visit 4: $t_{(23)} = -0.786$, $p = 0.631$, Visit 5: $t_{(25)} = 1.089$, $p = 0.286$) after correcting for multiple comparisons, suggesting minimal or no consistent coil drifting across trials within a given block (Supplementary Fig. 7C). Using group average MEP amplitudes for each power and phase combination across visits, we also performed ICC analysis to assess the consistency of MEP amplitudes within the groups across repeated measurements. ICC analysis revealed a significant correlation ($p = 0.008$) with moderate reproducibility (r = 0.5987) suggesting that observed trend for the phase dependent effects of mu-power on MEPs are reasonably consistent across visits.

3.4.2. Brain state effects on trial to trial variability of MEPs—

Finally, we examined phase dependent power effects on trial-to-trial MEP variability (Fig. 7A and B). For each subject, we computed standard deviation and interquartile range for each power-phase condition as metrics of variability across visits. No significant differences were observed both for standard deviation and interquartile range comparisons ($p > 0.05$), suggesting that trial-to-trial variability in MEP amplitudes do not change across phase-power conditions.

4. Discussion

Here, we systematically examined the modulatory effects of ongoing sensorimotor mu-oscillations on corticospinal excitability across five identical visits. We did not find any modulatory effect when MEPs were classified based on instantaneous sensorimotor mu-phase (trough vs peak) or pre-stimulus mu-power dynamics (high vs low) alone. Although,

instantaneous mu-power analyses showed that MEPs were larger at high-power trials compared to the low-power trials at the overall group level analyses (Fig. 4A), this effect was weak with relatively small effect size, and was not reproducible across visits. However, TMS pulses delivered at the negative peak of high magnitude muoscillations (high-trough) generated significantly larger MEP responses both at the overall group level analyses and across all visits independently, when compared to TMS pulses delivered at the positive peak and negative peak of low magnitude and positive peak of high magnitude mu-oscillations (high-peak), suggesting phase-dependent mu-power modulation on corticospinal excitability. More importantly, we showed that such phase-dependent power effects on corticospinal excitability were specific to sensorimotor mu-rhythms originating from the stimulated region and moderately reproducible across multiple visits at the group level. Our analyses provide convincing preliminary evidence that fluctuations in corticospinal excitability indexed by MEP amplitudes are partially driven by dynamic interactions between the magnitude and the phase of ongoing sensorimotor mu oscillations at the time of TMS, and may suggest promising insights for (re)designing neuromodulatory TMS protocols targeted to specific cortical oscillatory states.

High variability in consecutive MEPs elicited by identical TMS pulses is a well-documented phenomenon dating back to earliest TMS reports (Amassian et al., 1989; Brasil et al., 1992; Britton et al., 1991; Hess et al., 1987; Kiers et al., 1993). In one of these early reports, for example, Amassian and colleagues (Amassian et al., 1989) concluded that large fluctuations in MEP amplitudes between consecutive trials could not be attributed to minor deviations from the stimulation target or to the specific phases of cardiac and respiratory cycles. In their 1993 report, Kiers and colleagues (Kiers et al., 1993) confirmed these findings and suggested spontaneous fluctuations in neuronal excitability of both cortical circuits and spinal motoneurons as possible physiological mechanisms contributing to variability in MEP responses. Although several animal reports (Arieli et al., 1996; Haegens et al., 2011b; Klimesch, 2012; Van Kerkoerle et al., 2014) and human cognition studies (Zumer et al., 2014) also provided ample evidence for the role of ongoing neural oscillations on stimulus-evoked responses, human studies probing cortical networks with TMS have largely ignored the likely interactions between stimulus properties and instantaneous oscillatory brain states at the time of stimulation until recently. Recent studies investigating the role of instantaneous neural oscillations on human corticospinal excitability have predominantly focused on mu-rhythms (Bergmann, 2018; Bergmann et al., 2019; Hussain et al., 2019; Karabanov et al., 2021; Madsen et al., 2019; Schaworonkow et al., 2018, 2019; Schilberg et al., 2021; Zrenner et al., 2018) as animal studies showed correlated changes between cortical excitability and specific phases of sensorimotor mu-rhythms with consistently increased neuronal spiking rates at negative peaks of alpha oscillations (Haegens et al., 2011b). When we consider the oscillatory mu-phase alone and disregard the dynamic interactions between phase and magnitude of ongoing mu-rhythms, our results did not revealed any significant modulatory effect of mu-phase, with negligibly higher MEP amplitudes at the negative mu-phase (Fig. 3D). Instantaneous mu-power showed weak modulatory effect at the overall group level with larger MEPs at high-power trials, but this effect did not survive across individual visits. These results confirm some recent EEG-guided TMS studies conducted with non-preselected individuals (Hussain et al., 2019; Madsen et al., 2019) while

contradicting others showing significantly larger MEPs when TMS is given at the negative peak compared to the positive peak of mu-oscillations in a selected group of subjects based on the magnitude of their mu power expressed in the sensorimotor cortex (Zrenner et al., 2018). It is highly possible that powerful sensorimotor mu-oscillations in these pre-selected individuals in Zrenner et. Al (Zrenner et al., 2018) (12 out of 29) contributed to the observed significant differences in MEP amplitudes as a function of mu-phase which, similar to our results, otherwise might not have been observed at the group level if all participants (n = 29) would have been included. Indeed, when we classified MEPs considering mu-phase and power interactions, we observed a very similar pattern reported in Zrenner et al. (2018) with larger MEPs at mu-trough and smaller MEPs at mu-peak trials compared to null MEPs, and with significant differences between high-trough and high-peak MEPs (Fig. 5C). Importantly, we showed that this pattern is consistent at the group level across five independent visits suggesting reproducible modulation of corticospinal excitability by magnitude of ongoing sensorimotor mu-oscillations in a phase-dependent manner.

Based on animal preparations (Haegens et al., 2011b) and cognitive-perceptual performance tasks in humans (Klimesch, 2012; Zumer et al., 2014), it has been suggested that larger alpha oscillations depress neural processing rhythmically once per cycle by a functional mechanism called pulsed-inhibition (Mathewson et al., 2011). In line with the pulsed-inhibition hypothesis, we noted a suppression trend in MEPs at the peak of high magnitude mu-oscillations in our study, but significantly larger MEPs at the trough of high magnitude mu-oscillations strongly supported pulsed-facilitation of the neural excitability in the sensorimotor cortex. These results are also comparable to recent online TMS-EEG studies showing slightly reduced MEP amplitudes (Bergmann et al., 2019) with increased resting motor thresholds (Stefanou et al., 2020) at positive mu-peaks but larger MEPs and reduced resting motor thresholds at negative mu-peaks in individuals with relatively high magnitude sensorimotor mu-oscillations. Reproducibility of phase-dependent MEP modulations observed in our study also suggests robustness of pulsed-facilitation mechanisms such that ongoing sensorimotor mu-rhythms provide phasic windows of corticospinal excitability with enhanced neural responsivity to TMS at sensorimotor-mu valleys. These results, together with the recent reports, suggest that brain-state dependent (TMS) applications may be promising paradigm for addressing high inter and intra-subject variability in non-invasive brain stimulation protocols.

Indeed, brain-state dependent (TMS) application has quickly become a new trend both in experimental and clinical research paradigms, with promising initial results. Studies with single-pulse designs showed that TMS delivered at the trough phase of ongoing mu oscillations over the motor cortex induced stronger interhemispheric connectivity (Momi et al., 2022) and enhanced offline motor skill learning (Hussain et al., 2021). Over the years, the use of various repetitive TMS (rTMS) protocols, for example, has risen considerably to modulate cortical activity (Di Lazzaro et al., 2011) and human cognition (Chung et al., 2019). Given the substantial inter- and intra-subject variability in rTMS induced corticospinal (Boucher et al., 2021; López-Alonso et al., 2014) or cortical modulation (Ozdemir et al., 2021), and poor reproducibility of rTMS induced neuromodulation with existing protocols (Ozdemir et al., 2021), synchronizing temporal patterns of the TMS trains to specific phases of ongoing oscillations at the individual level may be an important

paradigm shift to maximize effectiveness of rTMS-induced neuromodulation, its behavioral outcomes and reproducibility. In a series of promising studies, for example, it has been reported that an identical rTMS train delivered at repeating cycles of high versus low cortical excitability states results in opposite changes in lasting corticospinal and cortical plasticity (Zrenner et al., 2018), offline enhancement of working memory (Gordon et al., 2022), and stronger entrainment of brain oscillations (Faller et al., 2022). It should be, however, noted that some of these initial reports are missing essential control conditions, such as the lack of comparisons for phase-based vs conventional stimulation protocols in Zrenner et al. (2018), Baur et al., 2020 and Hussain et al., 2021. More importantly, reproducibility and generalizability of such phase-dependent rTMS-induced neuromodulation is yet to be established.

We acknowledge certain limitations of the present work. First, our offline design with post-hoc trial sorting approach resulted in substantially different number of MEP trials between subjects within a given session and between separate sessions within a given subject across phase and power conditions. This issue was unavoidable, as we did not synchronize TMS pulses to ongoing sensorimotor oscillations, thus our offline design did not allow us to analyze data using within subject design to inspect individual trends within and across the sessions. Instead, we first normalized MEP amplitudes for each individual and analyzed data at the group level similar to several previous reports performing group level analyses (Bergmann et al., 2019; Schilberg et al., 2021). Although we are not able to generalize our findings to individual subjects, we believe current results reveal valuable information as this is the first study systematically examining mu-phase, mu-power and mu-phase and power interactions across five independent sessions to report reproducibility of brain-state effects on corticospinal excitability. Second, our subjects across all visits are young and healthy individuals with no known neurological, psychiatric or motor disorders. It is important to test generalizability of mu-rhythm based brain-state effects on corticospinal excitability with different age groups (e.g. children, older adults) and various neurological populations (e.g. Alzheimer's, Parkinson's) for extending practical and clinical implications of the current results.

Taken together, our data indicated reliable modulation of corticospinal excitability based on the properties of ongoing sensorimotor muoscillations but results should be interpreted with caution. Although, for example, there is a consistent pattern for mu-phase and power based modulation of cortical excitability across visits, brain-state dependent modulatory effects were not too large as normalized MEPs amplitudes ranged from +~16% (high-peak) to −~10% (high-trough) of null MEPs, suggesting that overall corticospinal excitability may vary approximately ±13% as a function of sensorimotor mu-oscillation dynamics (Fig. 5C). Whether such amount of modulation would be meaningful across experimental groups in basic research paradigms or would lead to better therapeutic outcomes in clinical applications is yet to be determined. Most importantly, MEP amplitudes were still highly variable across trials, conditions and subjects with increased variability in high-trough trials (Fig. 7A and B). This is important to consider in future studies as it shows that although state-dependent stimulation may modulate corticospinal excitability to a certain degree, it does not standardize fluctuations in consecutive TMS evoked MEP responses, and thus does not provide a solution to the problem of substantial MEP variability across

trials and subjects. Despite significant technological advancements, such as the use of neuronavigation (Jung et al., 2010) in TMS applications, and attempts to control for number of methodological (e.g. stimulus intensity, duration, stimulation device) and subjective (e.g. menstrual cycle, time of the day, attention, caffeine intake) factors, substantial MEP variability between and within-subjects still persists, and therefore limits the utility of corticospinal excitability as a reliable clinical and experimental tool, at least when indexed with the amplitude of MEPs. Future studies are needed to systematically examine a series of individual, experimental, and methodological factors influencing MEP amplitude variability, to test if MEP amplitudes can be stabilized within and between individuals, and thus whether MEPs can be used as a reliable metric of non-invasive brain stimulation in experimental and clinical research.

Supplementary Material

Refer to Web version on PubMed Central for supplementary material.

Declaration of competing interest and Acknowledgement

The authors declare the following financial interests/personal relationships which may be considered as potential competing interests: A. Pascual-Leone is a co-founder of Linus Health and TI Solutions AG; serves on the scientific advisory boards for Starlab Neuroscience, Magstim Inc., Hearts Radiant, TetraNeuron and MedRhythms; and is listed as an inventor on several issued and pending patents on methods and applications for noninvasive brain stimulation, and the real-time integration of noninvasive brain stimulation with electroencephalography and magnetic resonance imaging. None of these companies or interests influenced in any way the work reported. We are grateful to all research assistants who helped to run the study visits. Dr. Pascual-Leone is supported by grants from the National Institutes of Health (R24AG06142, and P01 AG031720), the National Science Foundation, and the Barcelona Brain Health Initiative funded primarily by La Caixa. Dr. Shafi is supported by the Football Players Health Study (FPHS) at Harvard University, and the National Institute of Health (R01 MH115949, R01AG060987, P01 AG031720-06A1). The content of this paper is solely the responsibility of the authors and does not necessarily represent the official views of Harvard University and its affiliated academic health care centres, or the National Institutes of Health.

Data availability statement

Raw de-identified data files will be uploaded to National Institute of Mental Health archive in accordance with the rules of the local ethics committee. Matlab Codes for EEG and EMG preprocessing, Spectral Power analyses, Hilbert transform, and phase/power based MEP classifications will be provided by Recep A. Ozdemir (rozdemir@bidmc.harvard.edu) upon request.

References

Amassian VE, Cracco RQ, Maccabee PJ, 1989. Focal stimulation of human cerebral cortex with the magnetic coil: a comparison with electrical stimulation. Electroencephalogr. Clin. Neurophysiology Evoked Potentials Sect 74, 401–416.

Arieli A, Sterkin A, Grinvald A, Aertsen AD, 1996. Dynamics of ongoing activity: explanation of the large variability in evoked cortical responses. Science 273, 1868–1871. [PubMed: 8791593]

Baur D, et al. , 2020. Induction of LTD-like corticospinal plasticity by low-frequency rTMS depends on pre-stimulus phase of sensorimotor mu-rhythm. Brain Stimul. 13, 1580–1587. [PubMed: 32949780]

Berens P, 2009. CircStat: a MATLAB toolbox for circular statistics. J. Stat. Software 31, 1–21.

Bergmann TO, 2018. Brain state-dependent brain stimulation. Front. Psychol 9, 2108. 10.3389/fpsyg.2018.02108. [PubMed: 30443236]

Bergmann TO, Lieb A, Zrenner C, Ziemann U, 2019. Pulsed facilitation of corticospinal excitability by the sensorimotor μ-alpha rhythm. J. Neurosci 39, 10034–10043. 10.1523/JNEUROSCI.1730-19.2019. [PubMed: 31685655]

Bergmann TO, Molle M, Schmidt MA, Lindner C, Marshall L, Born J, Siebner HR, 2012. EEG-guided transcranial magnetic stimulation reveals rapid shifts in motor cortical excitability during the human sleep slow oscillation. J. Neurosci 32, 243–253. 10.1523/JNEUROSCI.4792-ll.2012. [PubMed: 22219286]

Boucher PO, Ozdemir RA, Momi D, Burke MJ, Jannati A, Fried PJ, Pascual-Leone A, Shafi MM, Santarnecchi E, 2021. Sham-derived effects and the minimal reliability of theta burst stimulation. Sci. Rep 11, 21170 10.1038/s41598-021-98751-w. [PubMed: 34707206]

Brasil Neto, J P, McShane LM, Fuhr P, Hallett M, Cohen LG, 1992. Topographic mapping of the human motor cortex with magnetic stimulation: factors affecting accuracy and reproducibility. Electroencephalogr. Clin. Neurophysiology Evoked Potentials Sect. 85, 9–16.

Britton TC, Meyer B-U, Benecke R, 1991. Variability of cortically evoked motor responses in multiple sclerosis. Electroencephalogr. Clin. Neurophysiology Evoked Potentials Sect 81, 186–194.

Chung SW, Sullivan CM, Rogasch NC, Hoy KE, Bailey NW, Cash RF, Fitzgerald PB, 2019. The effects of individualised intermittent theta burst stimulation in the prefrontal cortex: a TMS-EEG study. Hum. Brain Mapp 40, 608–627. [PubMed: 30251765]

Corp DT, Bereznicki HGK, Clark GM, Youssef GJ, Fried PJ, Jannati A, Davies CB, Gomes-Osman J, Kirkovski M, Albein-Urios N, Fitzgerald PB, Koch G, Di Lazzaro V, Pascual-Leone A, Enticott PG, 2021. Large-scale analysis of interindividual variability in single and paired-pulse TMS data. Clin. Neurophysiol 132, 2639–2653. 10.1016/j.clinph.2021.06.014. [PubMed: 34344609]

Delorme A, Makeig S, 2004. EEGLAB: an open source toolbox for analysis of single-trial EEG dynamics including independent component analysis. J. Neurosci. Methods 134, 9–21. [PubMed: 15102499]

Desideri D, Zrenner C, Ziemann U, Belardinelli P, 2019. Phase of sensorimotor μ-oscillation modulates cortical responses to transcranial magnetic stimulation of the human motor cortex. J. Physiol 597, 5671–5686. [PubMed: 31535388]

Di Lazzaro V, Dileone M, Pilato F, Capone F, Musumeci G, Ranieri F, Ricci V, Bria P, Di Iorio R, De Waure C, 2011. Modulation of motor cortex neuronal networks by rTMS: comparison of local and remote effects of six different protocols of stimulation. J. Neurophysiol 105, 2150–2156. [PubMed: 21346213]

Di Lazzaro V, Oliviero A, Profice P, Ferrara L, Saturno E, Pilato F, Tonali P, 1999. The diagnostic value of motor evoked potentials. Clin. Neurophysiol 110, 1297–1307. [PubMed: 10423196]

Ermolova M, Metsomaa J, Zrenner C, Kozák G, Marzetti L, Ziemann U, 2021. Spontaneous phase-coupling within cortico-cortical networks: how time counts for brain-state-dependent stimulation. Brain Stimul. 14, 404–406. 10.1016/j.brs.2021.02.007. [PubMed: 33610790]

Faller J, Doose J, Sun X, Mclntosh JR, Saber GT, Lin Y, Teves JB, Blankenship A, Huffman S, Goldman RI, George MS, Brown TR, Sajda P, 2022. Daily prefrontal closed-loop repetitive transcranial magnetic stimulation (rTMS) produces progressive EEG quasi-alpha phase entrainment in depressed adults. Brain Stimul. 15, 458–471.10.1016/j.brs.2022.02.008. [PubMed: 35231608]

Fregni F, Pascual-Leone A, 2007. Technology insight: noninvasive brain stimulation in neurology—perspectives on the therapeutic potential of rTMS and tDCS. Nat. Clin. Pract. Neurol 3, 383–393. [PubMed: 17611487]

Goetz SM, Luber B, Lisanby SH, Peterchev AV, 2014. A novel model incorporating two variability sources for describing motor evoked potentials. Brain Stimul. 7, 541–552. [PubMed: 24794287]

Gordon PC, Belardinelli P, Stenroos M, Ziemann U, Zrenner C, 2022. Prefrontal theta phase-dependent rTMS-induced plasticity of cortical and behavioral responses in human cortex. Brain Stimul. 15, 391–402. 10.1016/j.brs.2022.02.006. [PubMed: 35182810]

Haegens S, Händel BF, Jensen O, 2011a. Top-down controlled alpha band activity in somatosensory areas determines behavioral performance in a discrimination task. J. Neurosci 31, 5197–5204. [PubMed: 21471354]

Haegens S, Nácher V, Luna R, Romo R, Jensen O, 2011b. α-Oscillations in the monkey sensorimotor network influence discrimination performance by rhythmical inhibition of neuronal spiking. Proc. Natl. Acad. Sci. USA 108, 19377–19382. [PubMed: 22084106]

Hess CW, Mills KR, Murray NM, 1987. Responses in small hand muscles from magnetic stimulation of the human brain. J. Physiol 388, 397–419. [PubMed: 3079553]

Hjorth B, 1975. An on-line transformation of EEG scalp potentials into orthogonal source derivations. Electroencephalogr. Clin. Neurophysiol 39, 526–530. 10.1016/0013-4694(75)90056-5. [PubMed: 52448]

Hordacre B, Goldsworthy MR, Vallence A-M, Darvishi S, Moezzi B, Hamada M, Rothwell JC, Ridding MC, 2017. Variability in neural excitability and plasticity induction in the human cortex: a brain stimulation study. Brain Stimul. 10, 588–595. [PubMed: 28024963]

Hussain SJ, Claudino L, Bönstrup M, Norato G, Cruciani G, Thompson R, Zrenner C, Ziemann U, Buch E, Cohen LG, 2019. Sensorimotor oscillatory phase–power interaction gates resting human corticospinal output. Cerebr. Cortex 29, 3766–3777. 10.1093/cercor/bhy255.

Hussain SJ, et al. , 2021. Phase-dependent offline enhancement of human motor memory. Brain Stimul. 14, 873–883. [PubMed: 34048939]

Jensen O, Mazaheri A, 2010. Shaping functional architecture by oscillatory alpha activity: gating by inhibition. Front. Hum. Neurosci 4, 186. [PubMed: 21119777]

Jung NH, Delvendahl I, Kuhnke NG, Hauschke D, Stolle S, Mall V, 2010. Navigated transcranial magnetic stimulation does not decrease the variability of motor-evoked potentials. Brain Stimul. 3, 87–94. [PubMed: 20633437]

Karabanov AN, Madsen KH, Krohne LG, Siebner HR, 2021. Does pericentral murhythm “power” corticomotor excitability? – a matter of EEG perspective. Brain Stimul. 14, 713–722. 10.1016/j.brs.2021.03.017. [PubMed: 33848678]

Kiers L, Cros D, Chiappa KH, Fang J, 1993. Variability of motor potentials evoked by transcranial magnetic stimulation. Electroencephalogr. Clin. Neurophysiology Evoked Potentials Sect 89, 415–423. 10.1016/0168-5597(93)90115-6.

Klimesch W, 2012. Alpha-band oscillations, attention, and controlled access to stored information. Trends Cognit. Sci 16, 606–617. [PubMed: 23141428]

Kobayashi M, Pascual-Leone A, 2003. Transcranial magnetic stimulation in neurology. Lancet Neurol. 2, 145–156. [PubMed: 12849236]

Lahr J, Paβmann S, List J, Vach W, Flöel A, Klöppel S, 2016. Effects of different analysis strategies on paired associative stimulation. A pooled data analysis from three research labs. PLoS One 11, e0154880. [PubMed: 27144307]

Lefaucheur J-P, Andrá-Obadia N, Antal A, Ayache SS, Baeken C, Benninger DH, Cantello RM, Cincotta M, de Carvalho M, De Ridder D, 2014. Evidence-based guidelines on the therapeutic use of repetitive transcranial magnetic stimulation (rTMS). Clin. Neurophysiol 125, 2150–2206. [PubMed: 25034472]

Levy WJ, York DH, McCaffrey M, Tanzer F, 1984. Motor evoked potentials from transcranial stimulation of the motor cortex in humans. Neurosurgery 15, 287–302. [PubMed: 6090972]

Livingston SC, Ingersoll CD, 2008. Intra-rater reliability of a transcranial magnetic stimulation technique to obtain motor evoked potentials. Int. J. Neurosci 118, 239–256. [PubMed: 18205080]

López-Alonso V, Cheeran B, Río-Rodríguez D, Fernández-del-Olmo M, 2014. Interindividual variability in response to non-invasive brain stimulation paradigms. Brain Stimul. 7, 372–380. [PubMed: 24630849]

Madsen KH, Karabanov AN, Krohne LG, Safeldt MG, Tomasevic L, Siebner HR, 2019. No trace of phase: corticomotor excitability is not tuned by phase of pericentral mu-rhythm. Brain Stimul. 12, 1261–1270. 10.1016/j.brs.2019.05.005. [PubMed: 31133479]

Mathewson KE, Lleras A, Beck DM, Fabiani M, Ro T, Gratton G, 2011. Pulsed out of awareness: EEG alpha oscillations represent a pulsed-inhibition of ongoing cortical processing. Front. Psychol 2 10.3389/fpsyg.2011.00099.

McGraw KO, Wong SP, 1996. Forming inferences about some intraclass correlation coefficients. Psychol. Methods 1, 30.

Momi D, et al. , 2022. Phase-dependent local brain states determine the impact of image-guided transcranial magnetic stimulation on motor network electroencephalographic synchronization. The Journal of physiology 600, 1455–1490, 1471. [PubMed: 34799873]

Ozdemir RA, Boucher P, Fried PJ, Momi D, Jannati A, Pascual-Leone A, Santarnecchi E, Shafi MM, 2021. Reproducibility of cortical response modulation induced by intermittent and continuous theta-burst stimulation of the human motor cortex. Brain Stimul. 14, 949–964. 10.1016/j.brs.2021.05.013. [PubMed: 34126233]

Ozdemir RA, Tadayon E, Boucher P, Momi D, Karakhanyan KA, Fox MD, Halko MA, Pascual-Leone A, Shafi MM, Santarnecchi E, 2020. Individualized perturbation of the human connectome reveals reproducible biomarkers of network dynamics relevant to cognition. Proc. Natl. Acad. Sci. USA 10.1073/pnas.1911240117.

Pascual-Leone A, Tormos JM, Keenan J, Tarazona F, Cañete C, Catalá MD, 1998. Study and modulation of human cortical excitability with transcranial magnetic stimulation. J. Clin. Neurophysiol 15, 333–343. [PubMed: 9736467]

Pellegrini M, Zoghi M, Jaberzadeh S, 2018. The effect of transcranial magnetic stimulation test intensity on the amplitude, variability and reliability of motor evoked potentials. Brain Res. 1700, 190–198. 10.10l6/j.brainres.2018.09.002. [PubMed: 30194017]

Rogasch NC, Sullivan C, Thomson RH, Rose NS, Bailey NW, Fitzgerald PB, Farzan F, Hernandez-Pavon JC, 2017. Analysing concurrent transcranial magnetic stimulation and electroencephalographic data: a review and introduction to the open-source TESA software. Neuroimage 147, 934–951. 10.1016/j.neuroimage.2016.10.031. [PubMed: 27771347]

Rösler KM, Roth DM, Magistris MR, 2008. Trial-to-trial size variability of motor-evoked potentials. A study using the triple stimulation technique. Exp. Brain Res 187, 51–59. 10.1007/s00221-008-1278-z. [PubMed: 18231784]

Rossi S, Antal A, Bestmann S, Bikson M, Brewer C, Brockmöller J, Carpenter LL, Cincotta M, Chen R, Daskalakis JD, 2020. Safety and recommendations for TMS use in healthy subjects and patient populations, with updates on training, ethical and regulatory issues: expert Guidelines. Clin. Neurophysiol.: Off. J. Int. Fed. Clin. Neurophysiol 132 (1), 269–306. 10.1016/j.clinph.2020.10.003.

Rossini PM, Burke D, Chen R, Cohen LG, Daskalakis Z, Di Iorio R, Di Lazzaro V, Ferreri F, Fitzgerald PB, George MS, 2015. Non-invasive electrical and magnetic stimulation of the brain, spinal cord, roots and peripheral nerves: basic principles and procedures for routine clinical and research application. An updated report from an IFCN Committee. Clin. Neurophysiol 126, 1071–1107. [PubMed: 25797650]

Rothwell JC, Hallett M, Berardelli A, Eisen A, Rossini P, Paulus W, 1999. Magnetic stimulation: motor evoked potentials. Electroencephalogr. Clin. Neurophysiol. Suppl 52, 97–103. [PubMed: 10590980]

Sanger TD, Garg RR, Chen R, 2001. Interactions between two different inhibitory systems in the human motor cortex. J. Physiol 530, 307–317. [PubMed: 11208978]

Schaworonkow N, Caldana Gordon P, Belardinelli P, Ziemann U, Bergmann TO, Zrenner C, 2018. μ-Rhythm extracted with personalized EEG filters correlates with corticospinal excitability in real-time phase-triggered EEG-TMS. Front. Neurosci 12, 954. 10.3389/ihins.2018.00954. [PubMed: 30618580]

Schaworonkow N, Triesch J, Ziemann U, Zrenner C, 2019. EEG-triggered TMS reveals stronger brain state-dependent modulation of motor evoked potentials at weaker stimulation intensities. Brain Stimul. 12, 110–118. 10.1016/j.brs.2018.09.009. [PubMed: 30268710]

Schilberg L, Ten Oever S, Schuhmann T, Sack AT, 2021. Phase and power modulations on the amplitude of TMS-induced motor evoked potentials. PLoS One 16, e0255815. 10.1371/journal.pone.0255815. [PubMed: 34529682]

Silvanto J, Pascual-Leone A, 2008. State-Dependency of transcranial magnetic stimulation. Brain Topogr. 21, 1. 10.1007/sl0548-008-0067-0. [PubMed: 18791818]

Stefanou M-I, Galevska D, Zrenner C, Ziemann U, Nieminen JO, 2020. Interhemispheric symmetry of μ-rhythm phase-dependency of corticospinal excitability. Sci. Rep 10, 7853. 10.1038/s41598-020-64390-w. [PubMed: 32398713]

Van Kerkoerle T, Self MW, Dagnino B, Gariel-Mathis M-A, Poort J, Van Der Togt C, Roelfsema PR, 2014. Alpha and gamma oscillations characterize feedback and feedforward processing in monkey visual cortex. Proc. Natl. Acad. Sci. USA 111, 14332–14341. [PubMed: 25205811]

Wassermann E, 2002. Variation in the response to transcranial magnetic brain stimulation in the general population. Clin. Neurophysiol 113, 1165–1171. 10.1016/S1388-2457(02)00144-X. [PubMed: 12088713]

Zrenner C, Belardinelli P, Müller-Dahlhaus F, Ziemann U, 2016. Closed-Loop neuroscience and non-invasive brain stimulation: a tale of two loops. Front. Cell. Neurosci 10 10.3389/fncel.2016.00092.

Zrenner C, Desideri D, Belardinelli P, Ziemann U, 2018. Real-time EEG-defined excitability states determine efficacy of TMS-induced plasticity in human motor cortex. Brain Stimul. 11, 374–389. 10.1016/j.brs.2017.ll.016. [PubMed: 29191438]

Zrenner C, Galevska D, Nieminen JO, Baur D, Stefanou M-I, Ziemann U, 2020. The shaky ground truth of real-time phase estimation. Neuroimage 214, 116761. 10.1016/j.neuroimage.2020.116761. [PubMed: 32198050]

Zumer JM, Scheeringa R, Schoffelen J-M, Norris DG, Jensen O, 2014. Occipital alpha activity during stimulus processing gates the information flow to object-selective cortex. PLoS Biol. 12, e1001965. [PubMed: 25333286]

Key points

- Combining transcranial magnetic stimulation (TMS) with electromyography (EMG) and electroencephalography (EEG) can provide direct measurements to examine how instantaneous fluctuations in cortical oscillations contribute to variability in TMS-induced corticospinal responses.
- Here, we systematically examined modulatory effects of ongoing sensorimotor mu-oscillations on corticospinal excitability across five identical visits.
- TMS delivered at the negative peak of high magnitude muoscillations generated the largest MEP responses across all visits suggesting phase-dependent mu-power modulation on corticospinal excitability.
- Phase-dependent power effects on corticospinal excitability were specific to sensorimotor mu-rhythms originating from the stimulated region and reproducible across multiple visits.
- We provide further evidence that fluctuations in corticospinal excitability indexed by MEP amplitudes are partially driven by dynamic interactions between the magnitude and the phase of ongoing sensorimotor mu oscillations at the time of TMS.

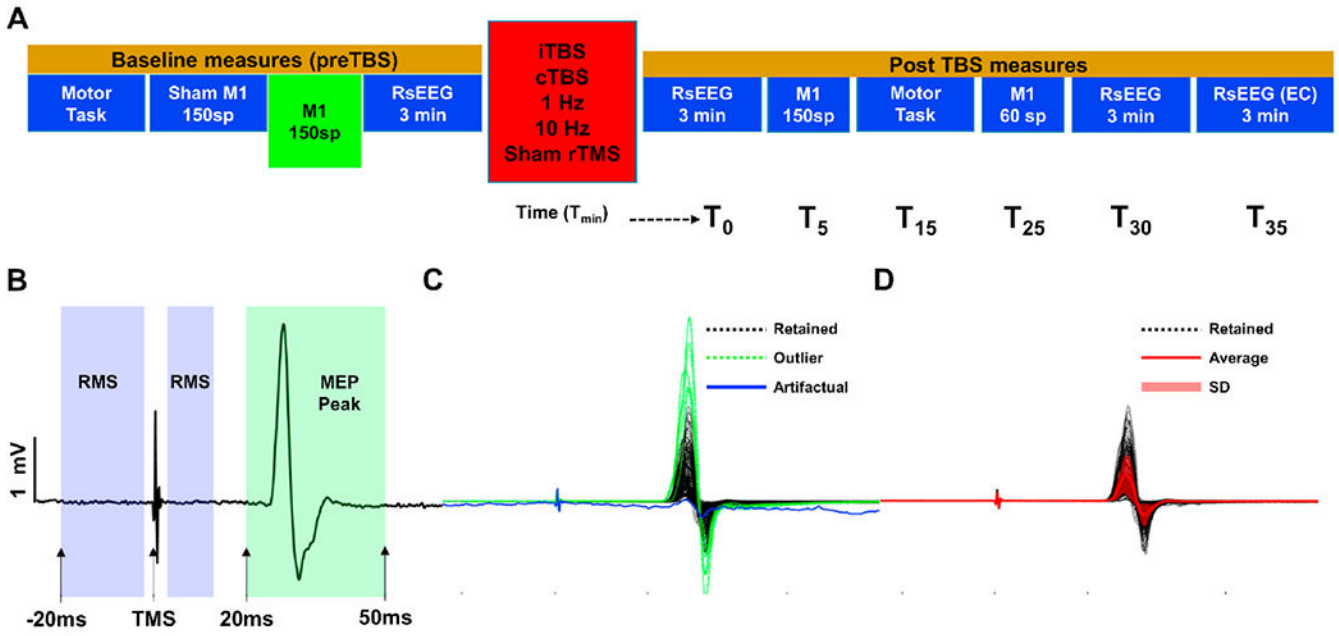

Fig. 1.

Study Design and Preprocessing of MEPs. A: Experimental design of the study protocol MEP data were taken from. Baseline M1 stimulation blocks (green block) with 150 single pulse TMS were used for all analyses. B: Representative MEP time series. Root mean square (RMS) is computed from purple shaded windows to identify artifactual trials and trials with high baseline EMG activity. MEP amplitude is computed as the absolute difference between signal maximum and minimum within the green shaded window. C: 150 MEP trials from a representative subject. Purple colored time series show rejected trials based on RMS calculation and green colored time series show outlier trials rejected based on standard deviation of MEP amplitudes. D: Retained trials after rejecting artifactual and outlier trials in C. Red colored time series show average MEP response of the block and red shaded regions represent standard deviation (1unit) of MEPs. (For interpretation of the references to color in this figure legend, the reader is referred to the Web version of this article.)

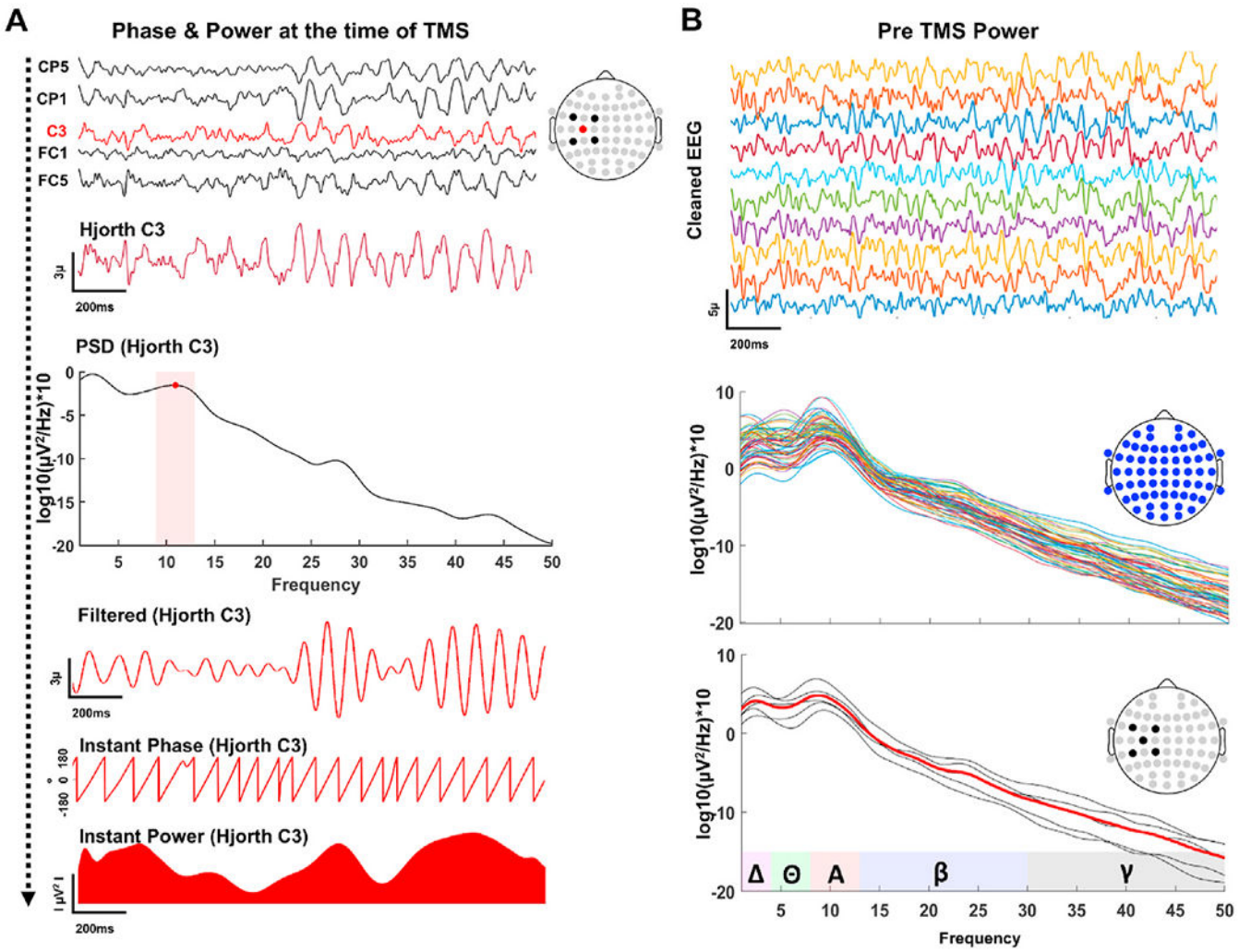

Fig. 2.

EEG Metrics. A: Selected preprocessed channels at the stimulation site (1st panel from the top) were hjorth-transformed centered around C3 (2nd panel from the top) and spectral power of the hjorth-transformed C3 was computed to find PAF (3rd panel from the top) for each individual. Hjorth-transformed C3 was then band-pass filtered (4th panel from the top) around PAF (±2Hz) followed by a Hilbert-transform to estimate instantaneous phase (5th panel from the top) and power (bottom panel) at the time of TMS. B: All preprocessed EEG channels (top panel) were used to compute spectral power density (middle panel) for individual epochs. Spectral power of the selected EEG channels at the site of the stimulation is averaged for each trial (lower panel) to estimate local power spectrum.

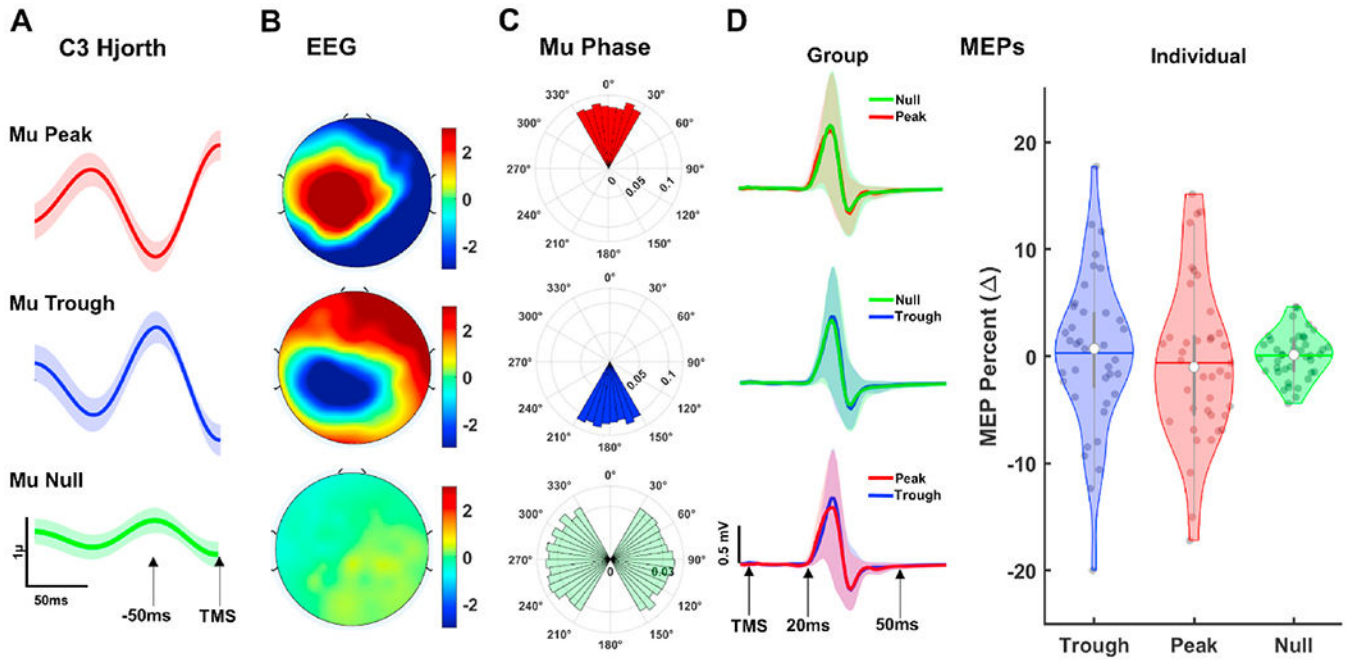

Fig. 3.

EEG Phase Estimation and Phase-based MEPs. A: Grand average Hjorth-transformed C3 time series for Peak (upper panel), Trough (middle panel), and Null phase (lower panel) trials. Shaded regions show standard error of measurement (1 unit). B: Scalp distribution of grand average EEG activity at the time of TMS across all trials and visits for Peak (upper panel), Trough (middle panel), and Null phase (lower panel) trials. C: Polar histograms showing angular distribution of the oscillatory phase estimation at the time of TMS for Peak (upper panel), Trough (middle panel), and Null phase (lower panel) trials. Radii values in polar histograms indicate ratio of individual MEP trials in each phase bin. D: Grand average MEP time series (left panels) across all visits and trials and violin plots (right panel) showing distribution of normalized MEPs averages for each subject across phase conditions. Shaded regions superimposed on time series (left panels) show standard error of measurement (±1 unit). White dots in violin plots represent median for normalized MEPs while gray colored dots show distribution of average MEPs for each subject. Colored horizontal lines and gray vertical bars represent grand average values and interquartile ranges, respectively.

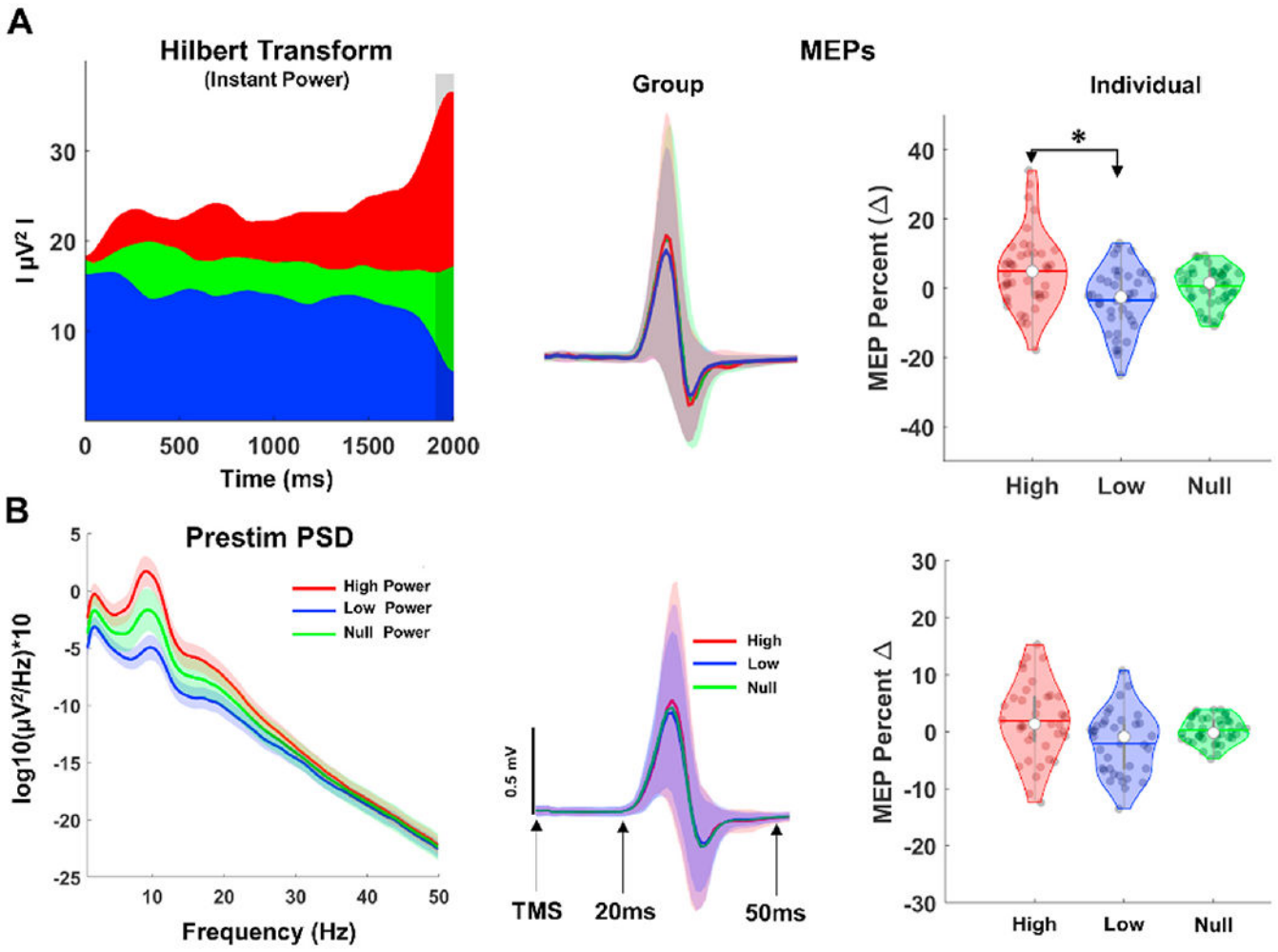

Fig. 4.

Instantaneous and Pre-stimulus EEG Power Estimation and Power-based MEPs. A: Grand average instantaneous power (left panel) and corresponding MEP time series (middle panel). Vertical gray shaded region in the power panel show time window (−100 to 0 ms) for computing instantaneous power at the time of TMS, and colored shaded regions in the MEP time series panel show standard error of measurement (±1 unit). B: Grand average PSD (left panel) of all trials and visits before TMS (−2000 to 0 ms) and MEP time series (middle panel). Violin plots (right panels) showing distribution of normalized MEPs for each subject across power conditions.

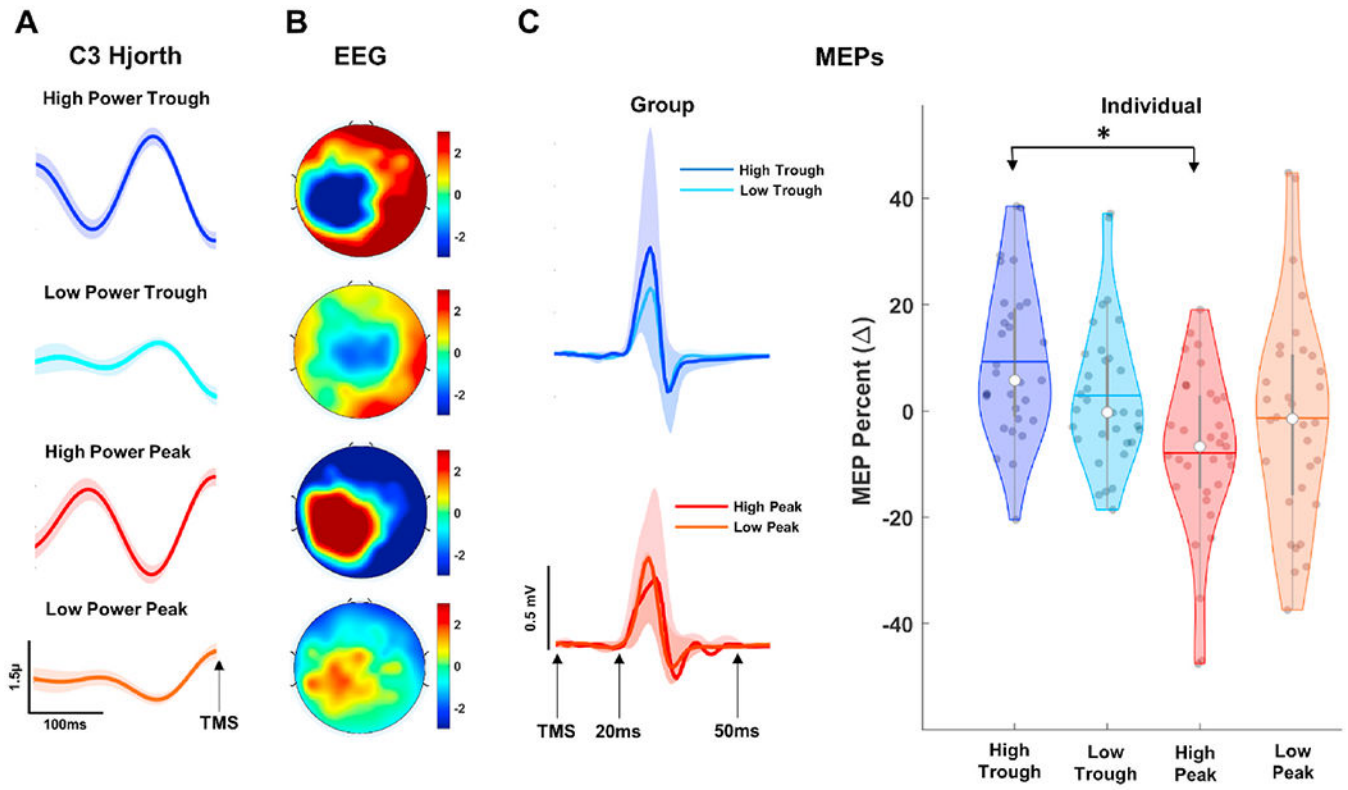

Fig. 5.

MEP Classification as a Function of EEG Phase and Power. A: Grand average Hjorth-transformed C3 time series for High-Trough (first panel from top), Low-Trough (second panel from top High-Peak (third panel from top), and Low-Peak (last panel). Shaded regions show standard error of measurement (1 unit). B: Scalp distribution of grand average EEG activity at the time of TMS across all trials and visits for combination of phase and power trials described in A. C: MEP time series (left panels) and violin plots (right panel) showing distribution of normalized MEPs for each subject across phase conditions. Shaded regions in left panels show standard error of measurement (±1 unit). White dots in violin plots represent median for normalized MEPs while gray colored dots show distribution of individual MEPs. Colored horizontal lines and gray vertical bars represent grand average values and interquartile ranges, respectively.

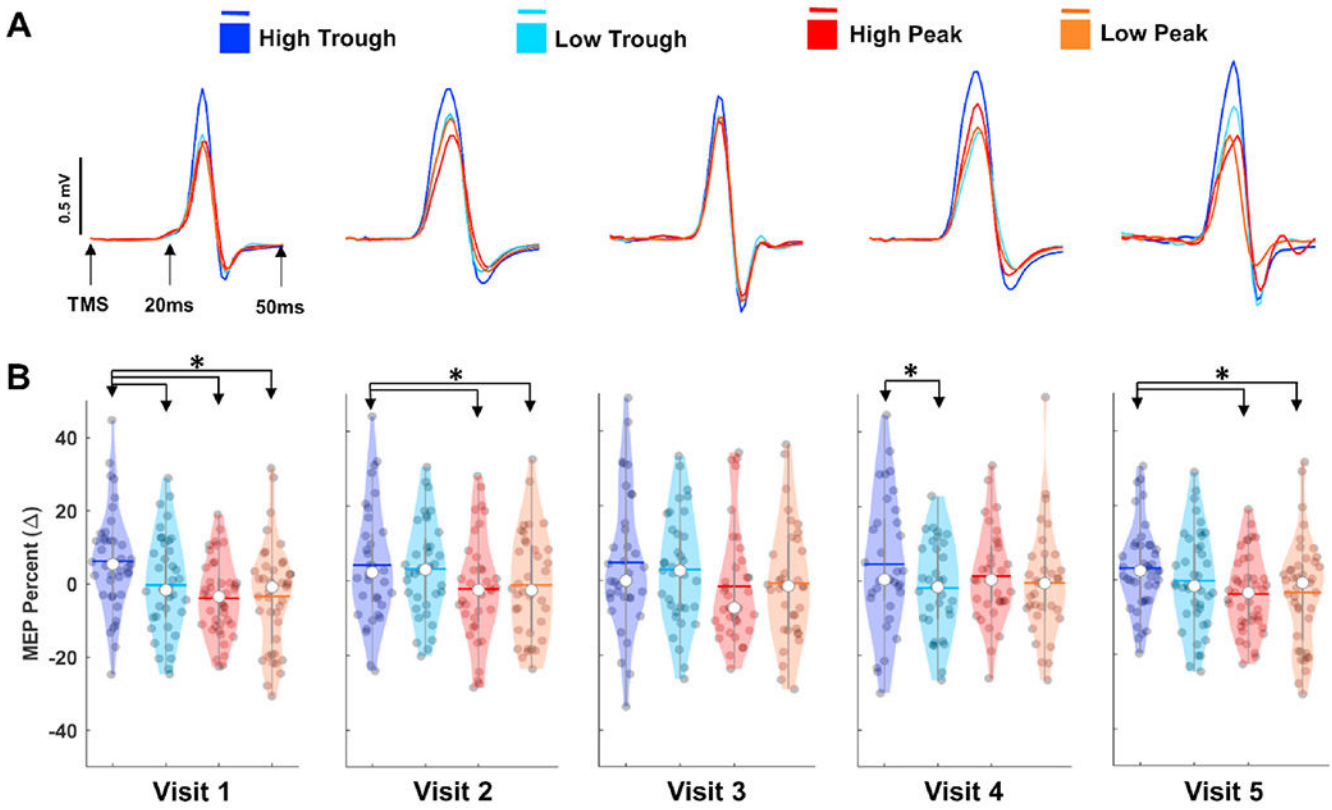

Fig. 6.

Reproducibility of Phase Dependent Power Effects on Motor Cortical Excitability. A: Color-coded average MEP time series for each visit as a function of mu phase and power at the time of TMS. B: Violin plots showing distribution average MEPs for each subject across conditions and visits. * denotes statistically different comparisons with Bonferroni correction. (For interpretation of the references to color in this figure legend, the reader is referred to the Web version of this article.)

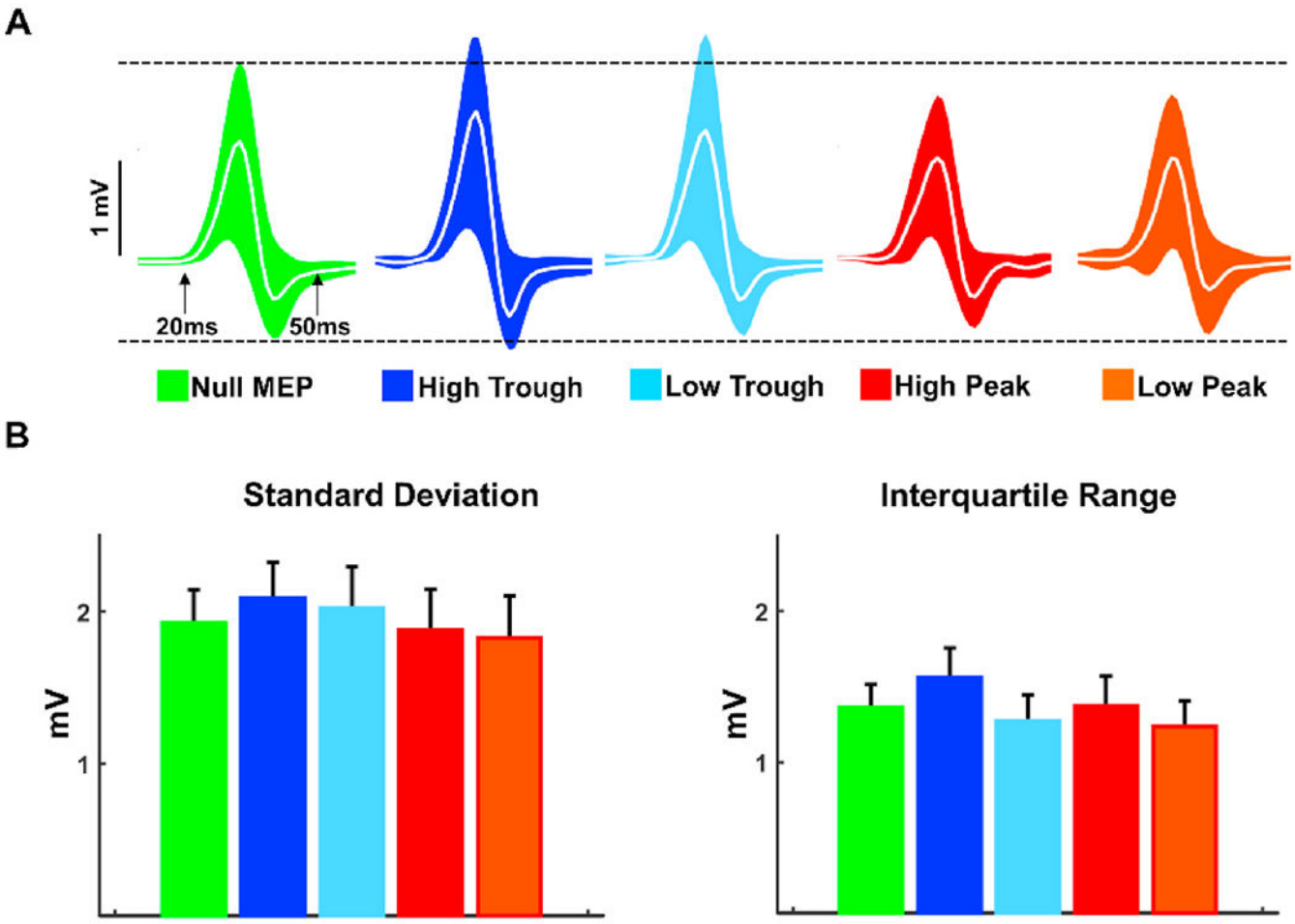

Fig. 7.

MEP Variability Across mu Phase and Power conditions. A: MEP time series across visits for each condition. Colored regions represent standard deviation (±1 unit) straight lines (white) show grand average. Black dotted lines were placed on the upper and lower edges of Null MEP trials as a reference for power and phase based conditions. B: Color-coded averages of subject level standard deviations (left panel) and interquartile ranges (right panel) of MEPs across visits. * denotes statistically different comparisons with Bonferroni correction. (For interpretation of the references to color in this figure legend, the reader is referred to the Web version of this article.)